

Article

Polyplex Formation Influences Release Mechanism of Mono- and Di-Valent Ions from Phosphorylcholine Group Bearing Hydrogels

A. Nolan Wilson ^{1,2}, Mark Blenner ² and Anthony Guiseppi-Elie ^{1,2,3,4,5,*}

¹ Center for Bioelectronics, Biosensors and Biochips (C3B), Clemson University Advanced Materials Center, 100 Technology Drive, Anderson, SC 29625, USA; E-Mail: anwilso@g.clemson.edu

² Department of Chemical and Biomolecular Engineering, 132 Earle Hall, Clemson University, Clemson, SC 29634, USA; E-Mail: blenner@clemson.edu

³ Department of Bioengineering, 132 Earle Hall, Clemson University, Clemson, SC 29634, USA

⁴ Holcombe Department of Electrical and Computer Engineering, 132 Earle Hall, Clemson University, Clemson, SC 29634, USA

⁵ ABTECH Scientific, Inc., Biotechnology Research Park, 800 East Leigh Street, Richmond, VA 23219, USA

* Author to whom correspondence should be addressed; E-Mail: guiseppi@clemson.edu or guiseppi@abtechsci.com; Tel.: +1-864-656-1712; Fax: +1-864-656-1713.

Received: 14 July 2014; in revised form: 3 September 2014 / Accepted: 9 September 2014 /

Published: 25 September 2014

Abstract: The release of monovalent potassium and divalent calcium ions from zwitterionic phosphorylcholine containing poly(2-hydroxyethyl methacrylate) (pHEMA)-based hydrogels was studied and the effects of polymer swelling, ion valence and temperature were investigated. For comparison, ions were loaded during hydrogel formulation or loaded by partitioning following construct synthesis. Using the Koshmeyer-Peppas release model, the apparent diffusion coefficient, D_{app} , and diffusional exponents, n , were $D_{app}(\text{pre-K}^+) = 2.03 \times 10^{-5}$, $n = 0.4$ and $D_{app}(\text{post-K}^+) = 1.86 \times 10^{-5}$, $n = 0.33$ respectively, indicative of Fickian transport. The $D_{app}(\text{pre-Ca}^{2+}) = 3.90 \times 10^{-6}$, $n = 0.60$ and $D_{app}(\text{post-Ca}^{2+}) = 2.85 \times 10^{-6}$, $n = 0.85$, respectively, indicative of case II and anomalous transport. Results indicate that divalent cations form cation-polyelectrolyte anion polymer complexes while monovalent ions do not. Temperature dependence of potassium ion release was shown to follow an Arrhenius-type relation with negative apparent activation energy of -19 ± 15 while calcium ion release was temperature independent over the physiologically relevant range (25–45 °C) studied. The negative apparent activation energy may be due to temperature dependent polymer swelling. No effect of polymer swelling on

the diffusional exponent or rate constant was found suggesting polymer relaxation occurs independent of polymer swelling.

Keywords: polyplexes; hydrogels; electromigration; release; transport; diffusional exponent

1. Introduction

Highly hydratable cross-linked polymers, or hydrogels, have become a mainstay in biological and biomedical applications [1] due to their desirable properties engendered by controllable high degree of hydration [2,3], cell and tissue biocompatibility [4] and high potential for molecular engineering [5] relative to other materials. A canonical example of a hydrogel, poly(2-hydroxyethyl methacrylate) (pHEMA), was first used in contact lenses for its optical clarity, dimensional stability, mechanical properties and biologically benign nature [6]. Since then, hydrogels have expanded in molecular repeat unit composition, architecture and applications to have technological impact in drug and biomolecule therapeutics [7], multiplexed biomolecular detection [8], biosensor-based molecular diagnostics [9], drug free macromolecular therapeutics [10] and tissue engineering and regenerative medicine [11]. Moreover, hydrogels are continually being molecularly engineered to serve as stimuli-responsive polymers [12] within their particular end-use environments by exploiting various sense and respond mechanisms [13–15]. More recently, feedback control has been integrated into bioresponsive hydrogels creating synthetic analogs to tightly regulated metabolic pathways [16,17]. While development, application and commercialization of hydrogels moves forward, fundamental understanding of their properties, interactions between the local bio-environment and the causal relationship between imbibed moieties and polymer structures are still an active area of research [14,18]. Controlled drug delivery is an area wherein fundamental understanding of hydrogel-drug interaction allows proper design of polymers and contributes to the successful development of drug delivery systems. The effects of hydrogel swelling dynamics; solute transport properties; *in situ* kinetics of enzymatic and/or binding recognition reactions; ionic interactions; and environmental (pH, temperature, ionic strength) changes can alter the performance of a biologically responsive system [15,19–21]. These factors greatly influence polymer design and could have unforeseen consequences on the release profiles of the delivered drugs, ultimately impacting safety and/or efficacy.

Work done by Korsemyer, Ritger, and Peppas pioneered methods to study and model drug delivery from polymeric hydrogel systems [22–24]. The culmination of this early work, using pHEMA as the drug delivery polymer, was the combination of two explicitly derived drug release models which describe diffusion controlled (Fickian or Case I) and polymer relaxation controlled (Case II) release; Equations (1) and (2), respectively. In general, polymeric hydrogels that do not exhibit appreciable relaxation or for which the polymer segmental relaxation time is much smaller than the characteristic diffusion time for solvent transport, experimentally display standard Fickian diffusion. In this case, solvent transport is controlled by a simple concentration gradient and water uptake by the polymeric hydrogel exhibits the characteristic $t^{1/2}$ dependence, with the resulting swelling also exhibiting $t^{1/2}$ dependence, Equation (1). When hydrogel segmental relaxation is the dominant mechanism involved in solvent transport, then a time-independent hydration is observed and the swelling will depend

linearly on time t , Equation (2). Mathematically, these two release mechanisms have been shown to be a function of $t^{1/2}$ and t (zero order), for planar hydrogel geometries, which can be used to differentiate release mechanisms based on experimental observation. Previous work by Alfrey *et al.* showed Equations (1) and (2) could be summed to describe the transport of two species into a polymer matrix, one controlled through Fickian diffusion and one controlled through polymer relaxation-driven swelling, resulting in Equation (3) [25]. Finally, the heuristic combination of terms in Equation (3) has resulted in a semi-empirical mathematical description, Equation (4), which has been shown to accurately predict drug release profiles from planar, cylindrical, and spherical geometries when $M_t/M_\infty < 0.60$. Additional utility of the model is gained since the value of the diffusional exponent, n , can indicate the predominant release mechanism; Fickian diffusion or polymer relaxation. The diffusional exponent has been shown to vary based on geometry and release mechanism as summarized in Table 1:

$$\frac{M_t}{M_\infty} = 4 \left[\frac{Dt}{\pi l^2} \right]^{1/2} = k_1 t^{1/2} \quad (1)$$

$$\frac{M_t}{M_\infty} = \frac{2k_0}{C_0 l} = k_2 t \quad (2)$$

$$\frac{M_t}{M_\infty} = k_1 t^{1/2} + k_2 t \quad (3)$$

$$\frac{M_t}{M_\infty} = k_{KP} t^n \quad (4)$$

where, M_t is the concentration of the released drug in the bathing solution at time t , M_∞ is the equilibrium concentration of the drug in the release solution, D is the diffusion coefficient, l is the slab thickness, k_1 is the diffusional rate constant which is proportionally related to D and l , k_0 is the polymer relaxation constant, C_0 is the initial concentration of the drug, k_2 is the swelling rate constant which is proportionally related to C_0 and l , k_{KP} is the Korsmeyer-Peppas rate constant and n is the diffusional exponent.

Table 1. Diffusional exponent values for various geometries and release mechanisms.

Slab	Cylinder *	Sphere	Release Mechanism
0.5	0.43	0.43	Fickian
$0.5 < n < 1.0$	$0.43 < n < 0.89$	$0.43 < n < 0.85$	Anomalous
1.0	0.89	0.85	Case II

* Indicates an aspect ratio of 2.25. Aspect ratio relation to n is provided in supplementary material.

Reprinted with permission from [23].

In many cases, however, rate balanced Fickian diffusion and polymer relaxation or the presence of a third component that contributes to overall system dynamics; e.g., an analyte for a sensor or a drug molecule for release, can result in an intermediate type of transport mechanism, which is referred to as anomalous transport [26]. To build upon previous work and expand the utility of the model developed by Korsmeyer, Ritger and Peppas, we [27,28] and others [29] have been investigating the transport of charged species within hydrogels. Of particular interest is ion transport within pHEMA-based hydrogels containing biomimetic, zwitterionic moieties such as phosphorylcholine. Phosphorylcholine,

the polar head group of the outer leaflet of cell membranes, has emerged as a biomimetic moiety for conferring cytocompatibility to hydrogels [30]. The study of ion transport within such hydrogels under test conditions that emulate physiological conditions could potentially inform various pathologies associated with ion transport across biological membranes. Moreover, ion transport within hydrogels is important in the design and application of wetting and disinfection agents for soft contact lenses, in controlling ocular drug delivery, in separation applications based on solute partitioning and in analytical techniques that employ hydrogel pre-concentration. Here the authors have investigated the effects of temperature, cation valence and swelling dynamics to determine the contribution of these factors to cation release kinetics.

To investigate the effect of valence, monovalent (potassium) and divalent (calcium) cations were released from a phosphorylcholine containing p(HEMA)-based hydrogel matrices. Such electrostatic migration is aptly described by the Nernst-Planck equation, Equation (5) [31]. Numerical solutions to the Nernst-Planck equation can be realized by coupling potential field effects through the Poisson equation, Equation (6) [31,32]. While finite element modeling approaches have been successful in reproducing experimental results to simplified systems using these equations, explicit relationships have not been resolved for the coupled transport phenomena. Experimental approaches are being taken to tease apart the importance of contributing phenomena to understand the role of charge density of the ion and hydrogel, the hydrodynamic radius of the ions involved, polymer relaxation dynamics and the molecular weight between crosslinks of the hydrogel that governs its mesh size:

$$\frac{\partial C_i}{\partial t} = \nabla \cdot (-D_{\text{eff},i} \nabla C_i - z_i \mu_{m,i} C_i \nabla \psi) + \nabla \cdot (C_i v) + r_i \quad (5)$$

$$\nabla^2 \psi = -\frac{F}{\epsilon_0 \epsilon_r} \sum_i^{N_f + N_b} (z_i C_i) \quad (6)$$

where C_i is the concentration of species i , D_{eff} is the effective diffusivity, z is the valence of the ion, $\mu = FD_{\text{eff}}/(RT)$ is the unsigned mobility, ψ is the electrical potential, v is the velocity of the solvent, r_i is the reaction term, F is Faradays constant, ϵ_0 is the permittivity in free space, ϵ_r is the dielectric constant, N_f and N_b are the numbers mobile and bound species, respectively.

To realize these distinctions, ions may be introduced into hydrogels during formulation alongside monomer and pre-polymer constituents prior to crosslinking (pre-synthesis loading). Alternatively, ions may be introduced into hydrogels by partitioning into the fully-hydrated, equilibrium-swollen hydrogel (post-synthesis loading). In addition, effects of temperature were investigated by monitoring ion release over a temperature range of 25–45 °C. In this work a 3 mol% tetraethyleneglycol diacrylate (TEGDA) cross-linked biomimetic poly(2-hydroxyethyl methacrylate) (pHEMA)-based hydrogel was synthesized to contain 2-methacryloyloxyethyl phosphorylcholine (MPC) units (1 mol%) and oligo(ethylene glycol) (400) monomethacrylate (OEG(400)MA) (5 mol%) cast into short cylindrical microforms. Both MPC and OEG constituents play a role in conferring biomimetic cytocompatibility to the hydrogel [33,34]. The transport of monovalent potassium cations (K^+) and divalent calcium cations (Ca^{2+}) was studied under two conditions. Firstly, ions in the form of the powdered chloride salt were loaded into the hydrogel during formulation and prior to UV crosslinking. Secondly, ions in the form of an aqueous solution of the chloride salt were partitioned into the blank hydrogel during

equilibrium hydration of the previously synthesized microform. Temperature dependent release of ions was studied at 25, 31, 37 and 45 °C using calibrated ion sensitive electrodes (ISEs).

2. Experimental Section

2.1. Reagents

Anhydrous calcium chloride (CaCl_2 , $\geq 99.99\%$) and potassium chloride (KCl , $\geq 99.0\%$) were purchased from Sigma-Aldrich (Milwaukee, WI, USA). The hydrogel components: HEMA, OEG(400)MA, the divalent cross linker, TEGDA, and the photoinitiator, 2,2-dimethoxy-2-phenylacetophenone (DMPA, 99%), were also purchased from Sigma-Aldrich. The biomimetic reagent 2-methacryloyloxyethyl phosphorylcholine (MPC) was prepared elsewhere as previously described [35]. The removal of polymerization inhibitors hydroquinone and monomethyl ether hydroquinone from the individual cocktail components proceeded by passing the liquid monomers over an inhibitor removal column. The buffer of 4-(2-hydroxyethyl)-1-piperazineethanesulfonic acid sodium salt (HEPES) was prepared to physiologically relevant conditions ($\text{pH} = 7.4$; ionic strength = 160 mM) [36]. HEPES buffer was firstly prepared to 100 mM and then titrated by the addition of sodium hydroxide (NaOH) to a concentration of 50 mM. Finally, the ionic strength of the buffer was adjusted by the addition of sodium chloride (NaCl) to a concentration of 160 mM. Deionized water (MilliQ DI, Billerica, MA, USA) was used to prepare all of the solutions.

2.2. Preparation of Monomer Cocktail and Synthesis of Hydrogel Discs

Hydrogel pre-polymer cocktails were prepared by combining monomer constituents in the mol% outlined in Table 2. To improve solubility, ethylene glycol and water were added to the mixture in a 1:1 (v/v) ratio such that the two species combined comprised 20 volume% of the formulation. After combining constituents, the mixture was ultrasonicated for 5 min and sparged with nitrogen to remove dissolved oxygen. Hydrogel discs were fabricated by placing silicone isolators (JTR12R-2.0, Grace Biolabs, Bend, OR, USA) onto trichloro(octadecyl)silane(OTS)-treated hydrophobic glass microscope slides and 31 μL of hydrogel pre-polymer was pipetted into the individual silicone isolation chambers and a second hydrophobic glass slide was placed on top of the silicone thereby sealing the liquid cocktail into the chambers between hydrophobic surfaces. The hydrogel-containing, sandwiched isolation chamber was immediately placed in a crosslinker (CX-2000, UVP, Upland, CA, USA) and UV irradiated at 366 nm for 10 min to initiate polymerization. The polymerized discs were then removed, retaining the form dimension of the chambers (thickness $l = 2.0$ mm and radius $a = 2.25$ mm), and stored at 4 °C until use. Figure 1A–C show a representation of the resulting macromolecular network structure, a hydrated hydrogel disc, and the sandwiched silicon isolation chamber, respectively.

Loading of the hydrogel discs with the salt species, CaCl_2 or KCl , proceeded through two methodologies. The first method, pre-loading, was achieved by dissolving the salts in the pre-polymer cocktail at a concentration of 100 mM. One pre-polymer mix was created for each salt. Dissolution of the salt was achieved by ultrasonication for 10 min followed by stirring overnight. The second method, post-loading, proceeded by bathing the hydrogel disc in a 100 mM solution of the respective salt at the

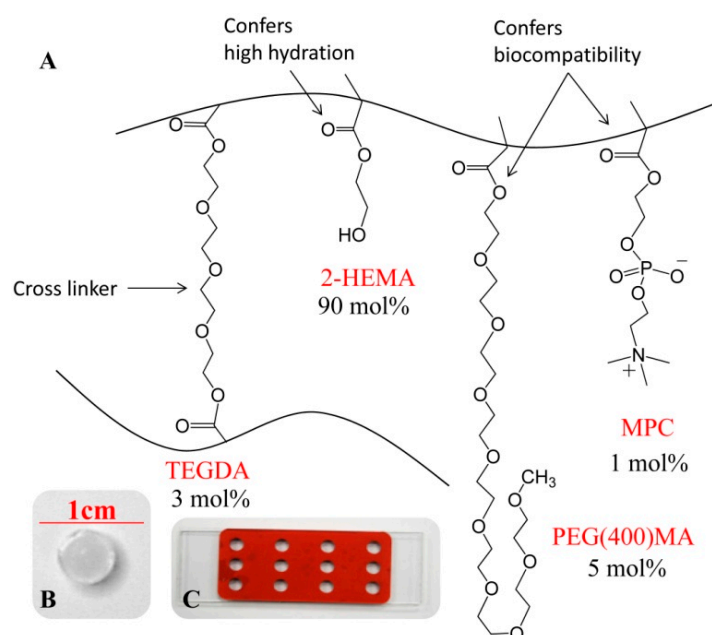
temperature of the release experiment. Hydrogel discs that were formulated to contain CaCl_2 and KCl for the pre-loading experiments were used in subsequent post-loading experiments, after the pre-loading experiment had occurred, and were only bathed in salt solutions that contained their respective preloaded salt. To ensure the polymer achieved equilibrium with the loading solution, hydrated disc weight was monitored hourly until the weight stabilized which took 2–4 h, typically.

Table 2. Hydrogel composition.

Hydrogel Constituent	Mol Percent of Hydrogel (%)
HEMA	90.0
TEGDA	3.0
PEG(400)MA	5.0 *
MPC	1.0
DMPA	1.0

* mol% calculated on the basis of the repeat unit concentration.

Figure 1. (A) Schematic of the molecular structure and mol% composition of the pre-polymer constituents of poly(HEMA)-based hydrogel possessing MPC, OEG(400)MA and cross-linked with 3 mol% TEGDA; (B) Hydrated hydrogel disc; and (C) Isolation chamber used for disc preparation sandwiched between two slides.



2.3. Experimental Setup for Release of Charged Species [27]

Prior to release, a calibration curve for each ion selective electrode (ISE) (Cole-Palmer ISE Electrode SC-27502-09 and YO-27504-26, Vernon Hills, IL, USA) was created by duplicate measurement of the voltage response to serial dilutions of CaCl_2 or KCl in HEPES buffer at each temperature, Appendix Figure A1. The calibration curve was used to convert voltage release data to concentration based on the Nernst equation. The voltage response from the ISE was collected using a Model DI-155 data acquisition interface (DATAQ Instruments, Inc., Akron, OH, USA) and associated software which recorded and ported the data to MS Excel. Release of the pre- or post-loaded Ca^{2+} or

K^+ cations was initiated by placing the loaded disc into a temperature equilibrated scintillation vial containing 3 mL of HEPES buffer and the appropriate ISE. To ensure ideal sink conditions, the release volume (100 times the disc volume) was constantly stirred during release and maintained at a constant temperature. Release experiments were performed in replicates of 3–6 per experimental setup.

2.4. Calibration and Performance of ISEs

ISEs are convenient for this type of ion release study as they generally have excellent response times, are quite stable and may be readily interfaced to data acquisition systems. However, ISEs do have a narrow temperature performance window. Accordingly, each ISE used was calibrated at each of the several temperatures of this study. Appendix Figure A1 shows the calibration curves obtained for duplicate runs over five decades of concentration at 25, 31, 37 and 45 °C. There is a clear linear trend of increasing slope expected for the behavior of ISEs; however, the slopes obtained did not comport with the expected Nernst value.

2.5. Hydrogel Characterization

Gravimetric hydrogel characterization was performed to determine Swelling% and Degree of Hydration (DoH) of the hydrogels in HEPES buffer or HEPES buffer containing different concentrations of the salt KCl or $CaCl_2$ between 25 and 45 °C. To calculate Swelling%, Equation (7), the hydrogel discs were weighed on a microbalance in their hydrated (H) and dehydrated (D) states. Swelling%, was determined immediately before and immediately after release of the ionic species at various temperatures by measuring the weight of the hydrogel disc at those times (S_b —before and S_a —after). The difference in Swelling% as a result of the release was determined from the before and after measurements and was calculated using Equation (8). DoH was calculated using Equation (9):

$$\text{Swelling\%} = \frac{M_{S_i} - M_D}{M_H - M_D} \quad (7)$$

$$\Delta \text{Swelling\%} = \frac{M_{S_a} - M_{S_b}}{M_H - M_D} \quad (8)$$

$$\text{DoH} = \frac{M_H - M_D}{M_H} \quad (9)$$

where M_H is the weight of the hydrated hydrogel in HEPES buffer, M_D is the weight of the dehydrated hydrogel and M_S is the weight of the hydrogel immediately before (M_{S_b}) or immediately after (M_{S_a}) release of the ionic species.

2.6. Analysis of Release Profiles

It was previously shown that release of Ca^{2+} and K^+ ions from TEGDA cross-linked p(HEMA)-based hydrogel containing phosphorylcholine groups was best represented by the Korsmeyer-Peppas model [27]. Accordingly, nonlinear least squared (NLLS) fits to Equation (4) were performed for all release profiles obtained. Data fitting used the portion of the release curve where $M_t/M_\infty < 0.60$. Statistical analysis was performed using Matlab (2012a) to determine statistical difference of parameters k_{KP} and n for loading, ion type and temperature groups. The analysis used

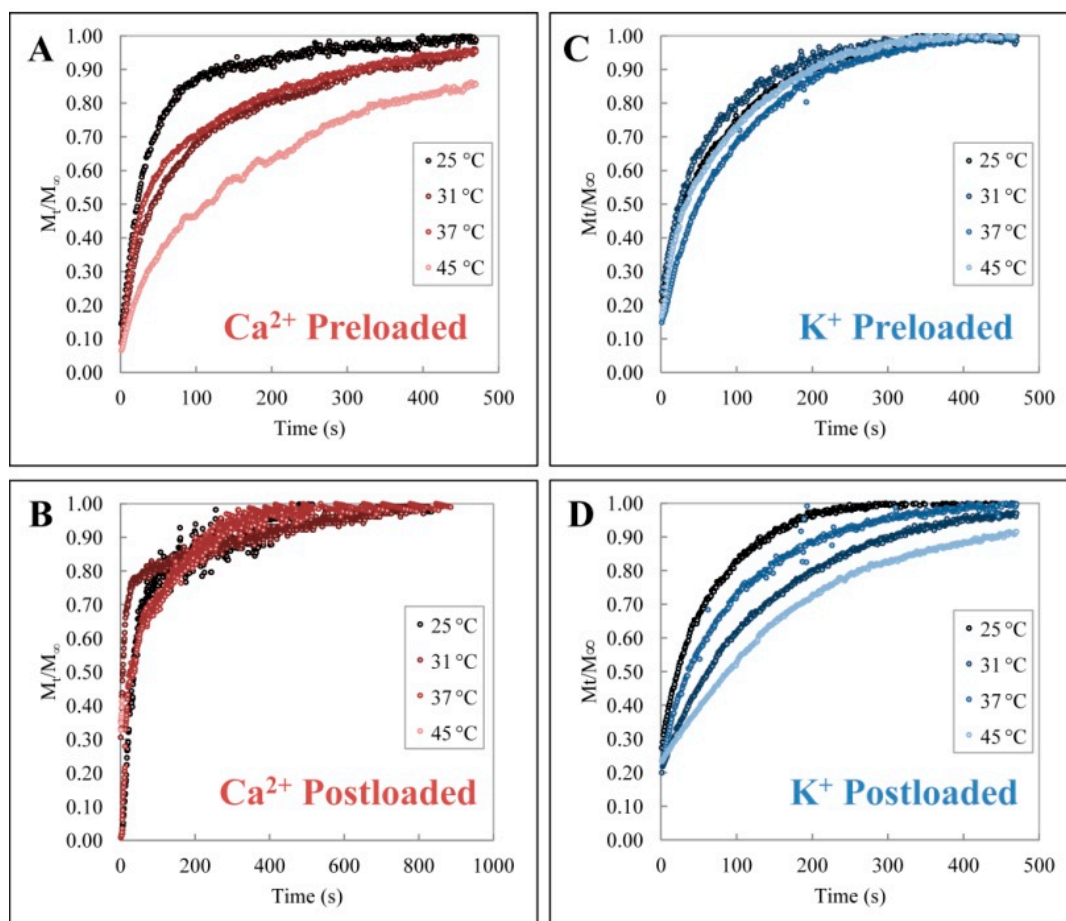
a nested ANOVA (analysis of variance) approach with temperature as a nested, random variable and ion type and loading method as the main, fixed variables. The nested design is provided in supplementary material, Appendix Table A1. Tukey HSD (honest significant difference) was used to determine if composite values of n were statistically different from each other and a multi-comparison test with the Bonferroni correction was used to determine if they were different from their theoretical values. Regression analysis was performed using MS Excel Data Analysis Tool Pack.

3. Results and Discussion

3.1. Release Profiles

Figure 2A–D show the normalized release profiles of calcium and potassium ions from pre-loaded and post-loaded hydrogels into pH 7.4 HEPES buffer at 25, 31, 37 and 45 °C. The molar concentration of the appropriate ion in the release solution at a given time, M_t , was determined from the acquired voltage vs. time data by use of the experimentally prepared calibration curves. The M_t value was normalized to the equilibrium ion concentration in the release solution, M_∞ , and plotted as a function of time for each temperature studied. Normalization was used to eliminate release dependence on the initial ion concentration in the hydrogel disc and for fitting to Equation (4).

Figure 2. Normalized release profiles of pre- (A,C) and post- (B,D) loaded Ca^{2+} (A,B) and K^+ (C,D) ions from pHEMA-based hydrogel discs.



3.2. Cation Effects on Release and Polymer Structure

The non-linear least squared fit of the release profiles with Equation (4) generated constants, n and k_{KP} , which were subsequently analyzed to determine the effect of cation valence on the release profiles. Composite values of the diffusional exponent, n , and the release rate constant, k_{KP} , were calculated for K^+ pre-loaded, K^+ post-loaded, Ca^{2+} pre-loaded and Ca^{2+} post-loaded gels. Figure 3A shows the results of these calculations where values of n for K^+ (blue bars) are clearly at or below the threshold for Fickian transport and values of n for Ca^{2+} (red bars) are clearly Case II and anomalous transport. To reinforce these graphically obvious findings, a multiple comparison (Tukey HSD) test was performed to determine the statistical difference between the several groups. At 95% confidence, it was shown that there was no statistical difference in the diffusional exponents for pre- vs. post-loaded hydrogels when potassium was the released ion while there was a statistical difference when calcium was the released ion ($p > 0.05$). Additionally, it was shown that values of n for K^+ and Ca^{2+} were statistically significantly different in both the pre- and post-loaded cases ($p < 0.05$). This indicates that cation valence clearly has a significant effect on the mechanism of release. A second multi-comparison (Least Significant Difference (LSD) with a Bonferroni correction) test showed that values of n for pre-loaded K^+ were not statistically different than 0.43 indicating that the hydrogels exhibited K^+ release profiles predicted by Fickian diffusion. Additionally, post-loaded K^+ release profiles resulted in values of n that were statistically lower than the Fickian value of $n = 0.43$. For post-loaded Ca^{2+} the diffusional exponent was not statistically different than 0.89 indicating the hydrogels with post-loaded Ca^{2+} exhibited release profiles that were consistent with a Case II type release behavior. Finally, the hydrogels possessing pre-loaded Ca^{2+} had n values that were found to fall between 0.43 and 0.89 indicating anomalous release behavior. Figure 3 shows the results of these statistical analyses. An alternate statistical analysis accounting for subsampling, nested ANOVA, supported these findings, Table 3.

Figure 3. (A) Composite diffusional exponent, n , values for different ion and loading. Where * indicates statistical significance ($p < 0.05$), ‡ indicates not statistically different than Fickian value of n (0.43) and † indicates not statistically different than Case II value of n (0.89); (B) Diffusional exponent values for hydrogels which do not (empty) and do (filled) contain MPC; and (C) Composite rate constant, k_{KP} , value for various ion and loading. Shaded region indicated range of k_{KP} values found elsewhere for water transport in hydrogels [37].

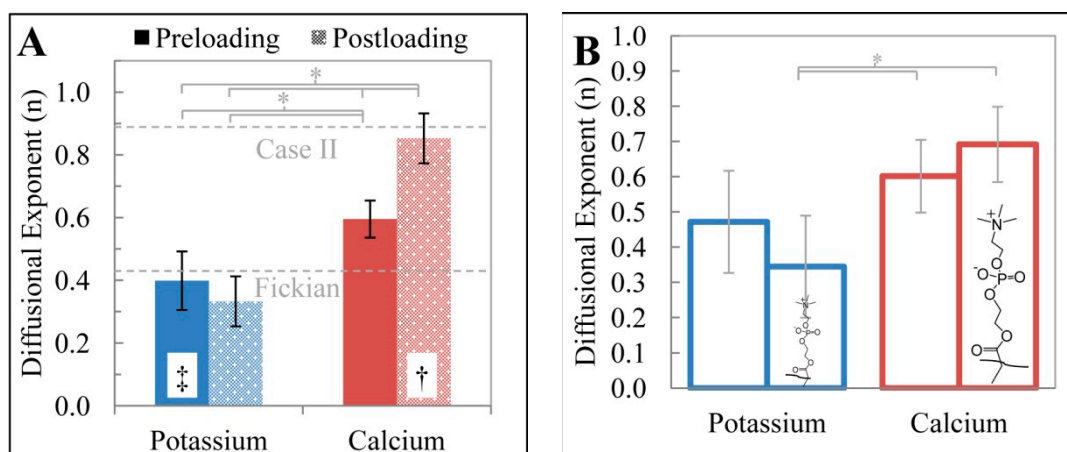


Figure 3. Cont.

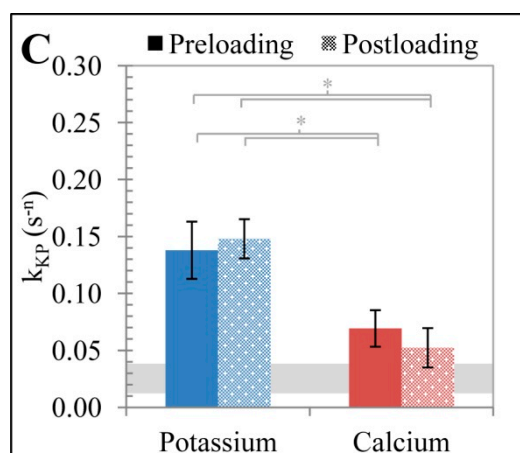


Table 3. Nested ANOVA (analysis of variance) for the effect of loading method, cation type and temperature on n and k_{KP} (where SS = sum of squares, d.f. = degrees of freedom, MS = mean of squares, F = f-statistic and $p = p$ -value).

Nested ANOVA for Diffusional Exponent (n)					
Source	SS	d.f.	MS	F	p
Loading	0.2371	1	0.2371	3.12	0.0970
Ion	3.1399	1	3.1399	41.28	0.0000
Temp (Loading, Ion)	1.0551	13	0.0812	1.74	0.0634
Error	4.5592	98	0.0465		
Total	8.7794	113			
Nested ANOVA for Rate Constat (k_{kp})					
Source	SS	d.f.	MS	F	p
Loading	0.0012	1	0.0012	0.18	0.6739
Ion	0.1763	1	0.1763	28.23	0.0001
Temp (Loading, Ion)	0.0892	13	0.0069	2.6	0.0038
Error	0.2583	98	0.0026		
Total	0.5187	113			

The dependence of n on ion valence suggests that the interaction between the mono- or di-valent ions and the zwitterion containing polymer are quite different and this interaction influences not just the release profile but the release mechanism. The interactions between the ions and polymer which affects the release profile may be understood with polymer swelling theory and polymer dynamics. The theory, developed by Flory and Huggins, originally described environmental effects of entropic polymer relaxation (rubber elasticity theory) [38,39] and free-energy dependent swelling (equilibrium solvation theory) [40]; however, it has been extended to include cationic, anionic and pH sensitive hydrogels [41]. The free energy of the system, ΔG , can be expressed as a function of the free energy of elastic deformation, ΔG_{el} , polymer-solvent mixing, ΔG_{mix} , and ionic contributions, ΔG_{ion} , Equation (10). Furthermore, the osmotic swelling pressure of a swollen polyelectrolyte gel, which is equal to the osmotic pressure of the solution at equilibrium, may be written as a function of the pressure contribution of these terms, Equation (11) [42,43]:

$$\Delta G = \Delta G_{\text{mix}} + \Delta G_{\text{el}} + \Delta G_{\text{ion}} \quad (10)$$

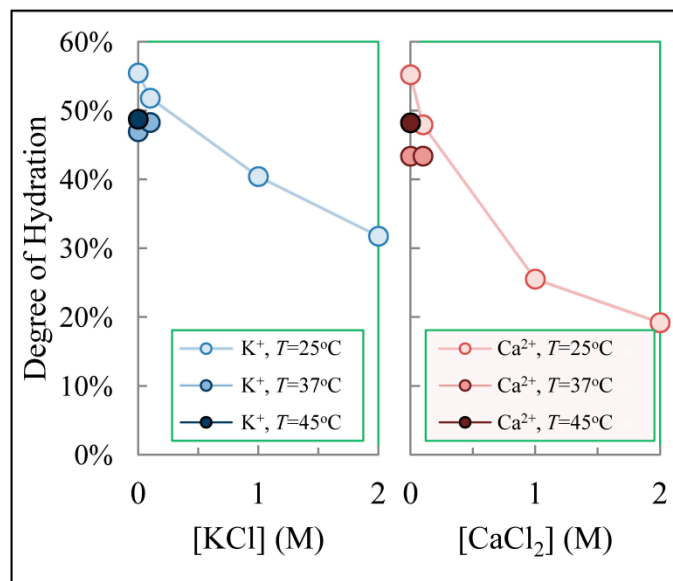
$$\begin{aligned} \Pi_{\text{gel}} &= \Pi_{\text{mix}} + \Pi_{\text{el}} + \Pi_{\text{ion}} \\ &= -\left(\frac{RT}{V_1}\right) [\ln(1 - \phi) + \phi + \chi\phi] + RTAv\phi^{1/3} + RT\left(\frac{i\phi}{V_m} + 2c_{\text{gel}} - 2c_{\text{sol}}\right) \end{aligned} \quad (11)$$

where R is the ideal gas constant, T is temperature, V_1 is the molar volume of the solvent, ϕ is the volume fraction of the polymer, χ is Flory-Huggins interaction parameter, A is a constant of order unity, v is the concentration of network chains, i is the fraction of charged monomers, V_m is molar volume of the monomer, and c_{gel} and c_{sol} are the concentrations of added salt in the gel and solution at equilibrium, respectively.

Work by Horkay *et al.* [43,44] used this theory to demonstrate the interaction of an anionic polyelectrolyte gel, sodium poly-acrylate cross-linked with N,N -methylenebis(acrylamide), with alkaline metal salts (LiCl, NaCl, KCl, and CsCl), alkaline earth metal salts (CaCl₂, SrCl₂, and BaCl₂) and rare earth metal salts (LaCl₃ and CeCl₃). The key findings of their work, applicable to ion release from zwitterionic hydrogels, were; (i) that the alkaline and alkaline earth metals do not contribute to the free energy of elastic deformation; subsequently, it was proposed that neither strongly interact to form cross-links with anionic pendent groups of the polymer; (ii) Through first and second order Flory–Huggins interactions parameters, it was shown that the alkaline metals do not contribute to the free energy of mixing, ΔG_{mix} , while the alkaline earth metals do contribute to this parameter. This implies that alkaline metals do not contribute to polymer-solvent interactions, and conversely, alkaline earth metals form polymer-ion complexes through charge-charge interactions between the divalent cations and the anionic polyelectrolyte. Studies of the sulfobetaine containing polymer, poly(N,N -dimethyl;(methacryloyloxyethyl) ammonium propane sulfonate) and sulfobetaine brushes [45–47] likewise show the independence of monovalent cation action. Similar observations were made for the swelling behavior of poly(MPC) that had been immersed in Li⁺, Na⁺, K⁺, Ca²⁺, Mg²⁺ and NH₄⁺ as the chloride salt. Here the poly(MPC), which showed enhanced swelling at pH < 2 and at temperatures $T > 60$ °C, showed only modest decrease in swelling up to 2 M cation concentration [48].

Diffusional exponent values reported here are consistent with the findings by Horkay *et al.* [43]. In both cases, hydrogels produce release profiles for K⁺ ions reflective of Fickian diffusion and which are expected for non-interacting entities being released from a hydrogel. On the other hand, Ca²⁺ release profiles demonstrate case II or anomalous release suggesting the influence of relaxation of ion-polymer complexes must occur for divalent cation release. Further evidence for this hypothesis is found from an investigation of the hydrogel degree of hydration. The DoH, which is related to ϕ , is presented as a function of the bathing salt concentration in HEPES, Figure 4. Hydrogels bathing in both KCl and CaCl₂ solutions exhibited salt concentration dependent reduction in DoH; however, hydrogels in the KCl solution retain more water than the gels in CaCl₂ as salt concentration was increased. The decrease in DoH for gels in KCl solution can be explained by the osmotic pressure of the salt, represented by the term Π_{ion} in Equation (11). Hydrogels in CaCl₂ solutions show a greater decrease in DoH as a function of salt concentration since swelling of the gels is affected by Π_{mix} in addition to Π_{ion} .

Figure 4. Degree of hydration for hydrogels as a function of the bathing solution salt concentration and temperature.



To investigate the possibility of an interaction between either of the two respective mono- and di-valent ions, potassium or calcium, and the zwitterionic MPC groups, pre-loaded hydrogels were formulated which did not contain MPC (0 mol% MPC) and the diffusional exponents were determined from their release profiles as previously described. A comparison of the n values obtained from hydrogels containing 0 mol% MPC and 1 mol% MPC is shown in Figure 3B. When the same ion was tested, there was no statistically significant difference between the values of n for hydrogels which contained 0 mol% MPC (empty bars) and 1 mol% MPC (filled bars). An examination of the diffusional exponents across cation valence but within the same polymer formulation revealed a statistically significant difference. The transport exponents for release from hydrogels which contained 1 mol% MPC but had different ions loaded into the polymer were significantly different. That is, the mechanism of release of K^+ and Ca^{2+} from 1 mol% MPC containing hydrogels was convincingly different. The K^+ ions were released by a Fickian transport mechanism while the Ca^{2+} ions were released by an Anomalous or Case II transport mechanism. Finally, a similar comparison was made for 0 mol% MPC hydrogels with the two different ions. In this case, there was not a statistically significant difference in the transport exponents. This indicates that both the presence of MPC and the valence difference between the two ions was required in order to establish a different release mechanism in pre-load hydrogels. It is believed that the presence of the Ca^{2+} ions facilitates the formation of the phosphorylcholine (PC) based polyplexes [43]. Due to its increased positive charge, it is hypothesized that the Ca^{2+} ion is able to interact more strongly with the partial negative charges of the zwitterionic PC groups. This is constituent with findings by Horkay as alkaline earth metals contributed to the free energy of mixing. The phenomenon of increased interaction between polymers and ions with greater positive charge does not appear to be limited to zwitterionic moieties; however, Figure 3A demonstrates that the contribution of the polymer can play a significant role.

As with the diffusional exponent, n , the rate constant, k_{KP} , was shown to be significantly different for ion valence (p value < 0.05) but not for loading methods, Figure 3C. That is, the loading method

did not appear to alter the mechanism of release. The values for k_{KP} do not fall within a range of values, 0.0028–0.0332 (s^{-n}), reported elsewhere for the transport of H₂O into pHEMA-based hydrogels at pH 7.0 [37]. In the cited study, the diffusional exponent was found to range from 0.369 to 0.556, indicative of a Fickian diffusion release mechanism. The comparison of the rate constants of between H₂O and K⁺ is of particular interest since the normalized released profiles are both linear with respect to $t^{1/2}$ but produce drastically different rate constants. A potential explanation for higher k_{KP} values for charged vs. neutral species may be found in the electromigration term. Currently, electromigratory effects under the influence of the ζ -potential of the microform, have not been put into the mathematical context of Equation (4), so behavior of n or k_{KP} via gradient potential release is not available; however, if diffusion and electromigration have similar theoretical transport exponents, the rate constants would become additive, Equation (12):

$$\frac{M_t}{M_\infty} = (k_F + k_E)t^{1/2} \quad (12)$$

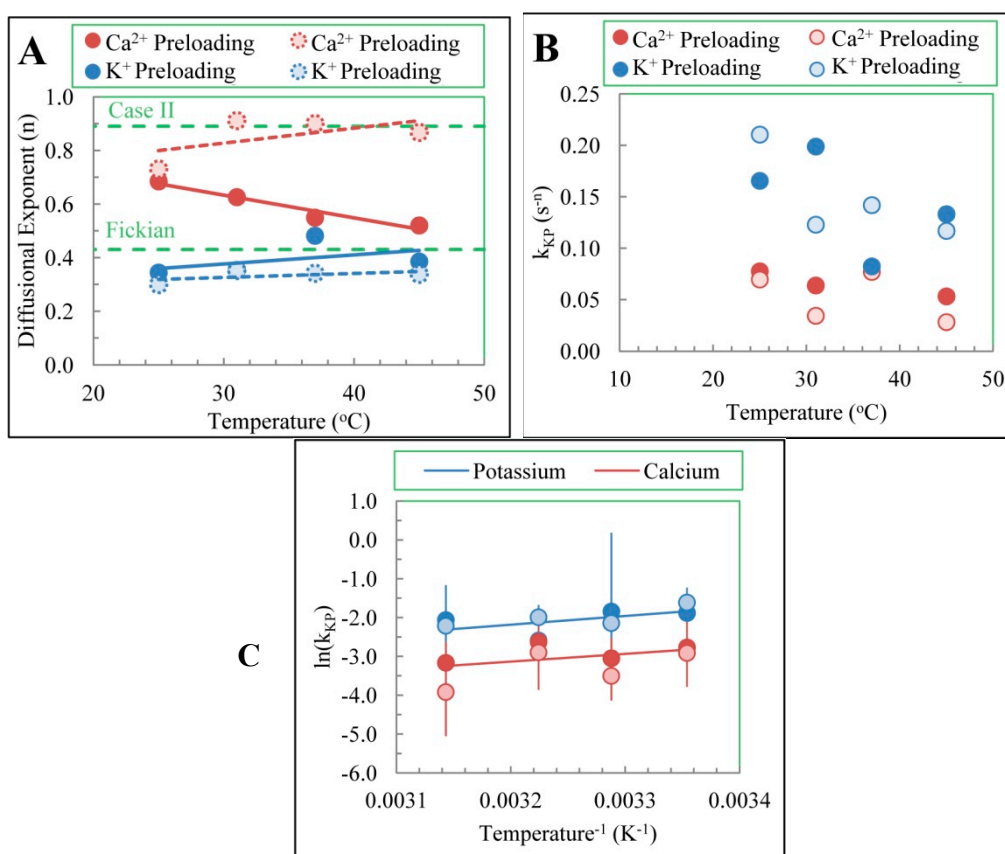
where k_F and k_E are the rate constants for Fickian diffusion and electromigration, respectively. The higher values of k_{KP} for K⁺ relative to H₂O could be explained by the additional driving force of electromigration if these effects are additive. Ca²⁺ has a value of k_{KP} between K⁺ and H₂O. Since Ca²⁺ release mechanism is Case II or Anomalous, the contribution of electromigration to k_{KP} may be attenuated as it follows $\cdot t^1$ rather than $\cdot t^{1/2}$ dependence. It is unclear if the different k_{KP} values are caused by the contribution of an electromigratory effect or other factors, such as polymer composition. Further mathematical relations and experimental work will need to be explored to investigate the effects of electromigration on the rate constant of release.

3.3. Temperature Dependence of Release

Figure 5A shows the diffusional exponent as a function of temperature for both cation type and loading method. Temperature dependence of n suggests the mechanism of release is thermally activated while temperature independence suggests the mechanism of release is not thermally activated over the temperature range studied. For hydrogels that were pre- or post-loaded with K⁺, a temperature independence, determined by regression analysis of the slope ($p > 0.05$), of n values was observed suggesting the mechanism of release is consistently Fickian over the temperature range. Temperature dependence of n values is observed for Ca²⁺ pre-loaded hydrogels ($p < 0.05$) which explains the previously discussed anomalous value of n reported for the composite of the values, Figure 3A. The value of the diffusional exponent for Ca²⁺ pre-loaded hydrogels is anomalous at low temperatures (25 and 31 °C) and moves towards a Fickian value for higher temperatures, 37 and 45 °C. This suggests that at lower temperatures there is not enough thermal energy to disrupt the cation and polyelectrolyte complexes. Placing the hydrogel disc into the buffered solution increases the chemical potential difference between the cation and its surrounding environment; subsequently, the complexation sites are relaxed releasing the cation into void spaces within the hydrogel where it then diffuses out. An increase in temperature correspondingly increases the thermal energy of the cation-polyelectrolyte complexes; at high enough temperatures the thermal energy will be enough to disrupt this interaction. This will create solvated Ca²⁺ cations that are not hindered by the PC polyplexes and therefore readily diffuse out producing a Fickian release profile. Notably, release of Ca²⁺ that were post-loaded into

hydrogels exhibit temperature independence ($p > 0.05$) and consistently exhibit n values consistent with Case II transport over the temperature range. Since the post-loading occurred through partitioning, it is possible that the majority of the loaded Ca^{2+} was incorporated into the hydrogel through complexation; conversely, the pre-loaded hydrogels did form substantial aggregation sites since the polymer chains and Ca^{2+} ions may have restricted mobility in the low hydration state of the polymer immediately following polymerization. This would reduce the number of complexation sites being relaxed during release and increase the amount of free Ca^{2+} available for release through a hindered-Fickian mechanism.

Figure 5. (A) Diffusional exponent, n , as a function of temperature; (B) Rate constant, k_{KP} as a function of temperature; and (C) Arrhenius plots of D_{eff} and k_{KP} for potassium and calcium, respectively.



Temperature dependence of k_{KP} was investigated through analysis of Arrhenius plots. Figure 5B shows a decrease in the value of k_{KP} with increasing temperature for K^{+} release while the value of k_{KP} remains constant with temperature for Ca^{2+} release [27]. The unaltered k_{KP} values were used in the Arrhenius plots. Apparent activation energies for release of K^{+} and Ca^{2+} were determined from the slope of the Arrhenius plots, Figure 5C, and were calculated to be -19 ± 15 and -17 ± 20 kJ/mol, respectively.

Regression analysis of $\ln(k_{\text{KP}})$ vs. T^{-1} showed the slope for potassium was statistically different than zero ($p < 0.05$) while the slope for calcium was not statistically significantly different than zero ($p > 0.05$). This indicates that the calcium release does not demonstrate temperature dependence over the temperature range investigated while potassium release does have a temperature dependence over the same range. The decreasing k_{KP} values vs. temperature and the negative activation energy are of

interest as, it is known that diffusivity, calculated to be 2.03×10^{-5} and 3.90×10^{-6} cm²/s using Equation for pre-loaded potassium and calcium, respectively, [49] and mobility of charge carriers increase exponentially with temperature [50]. The source of the negative apparent activation energy is currently unclear; however, complexities arising from ion transport within the hydrogel may contribute to the phenomena. One potential explanation of the negative activation energy is offered by consideration of polymer swelling as a function of temperature. Figure 4 shows temperature dependence in the DoH for hydrogels bathing in KCl and CaCl₂ salts. While the dependence appears non-linear, hydrogels at 37 and 45 °C demonstrated a lower DoH than gels at 25 °C. Invoking a porous media model of transport, Equation (14), it is clear that D_{eff} is a function of DoH through void fraction, Equation (15) [15]. Since DoH of the hydrogel decreased as function of temperature, the effective diffusivities will correspondingly decrease which would result in a negative apparent activation energy. This consideration is clearer for K⁺ as it follows Fickian release; however, Ca²⁺ has additional effects of polymer interactions and subsequently is a more complex system which may explain the difference in the temperature dependence of the two ions. Trongsatitkul *et al.* observed similar negative activation energies for FITC (fluorescein isothiocyanate)-dextran release from PNIPAm (Poly(*N*-isopropyl acrylamide) and contributed the phenomena to a denser polymer at higher temperatures, similar to the explanation provided here, and adsorption/desorption processes which competed with Fickian diffusion for the available kinetic energy to activate the processes [51]:

$$D_{\text{eff}} = \pi L^2 \left(\frac{k_{\text{KP}}}{4} \right)^{1/n} \quad (13)$$

$$D_{\text{eff}} = K_{\text{P}} K_{\text{R}} D_0 \frac{\varepsilon}{\tau} \quad (14)$$

$$\varepsilon = \text{DoH}(\rho_{\text{HG}}/\rho_{\text{sol}}) \quad (15)$$

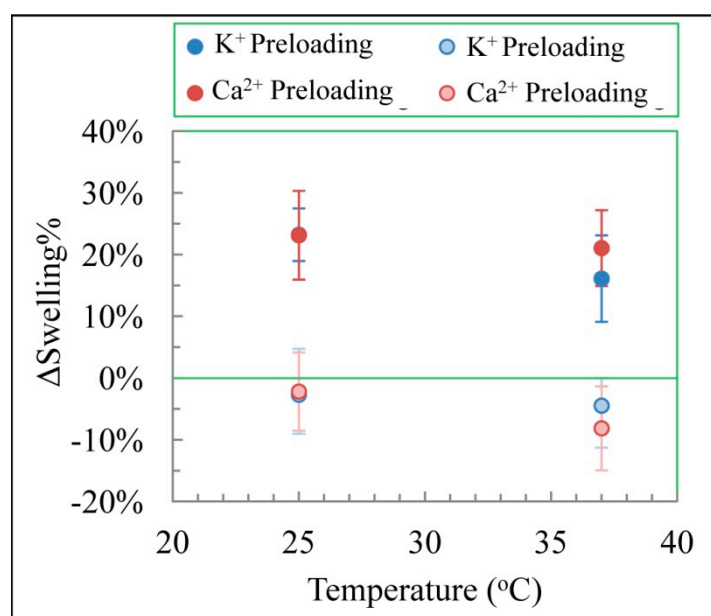
where K_{p} is the partitioning coefficient, K_{R} is the reflection coefficient, D_0 is the diffusivity in buffer, ε is polymer void fraction, τ is the tortuosity and ρ_{HG} and ρ_{sol} are the densities of the hydrogel and solution, respectively and $n = 0.43$. For ion transport, in order to maintain electro-neutrality within the hydrogel, as the ions are transported out of the hydrogel, their counter anions must simultaneously electromigrate. Since calcium is a divalent cation, twice as many counter anions must simultaneously electromigrate. This is in contrast to only one counter anion for the electromigration of potassium. While this is a simplified view, which may be justified in water and below the dilute solution limit, this model is rendered complicated by; (i) the distribution of appropriate voids within the hydrogel; (ii) the solvating influences of free and bound water within the hydrogel; (iii) the number, distribution and nano-architecture adopted by the charged moieties associated with the zwitterionic pendant groups of hydrogel; and (iv) the membrane potential gradient across the polymer-buffer interface. Since multiple processes may be contributing to these apparent activation energies a more complex model may be needed to interpret the values.

3.4. Hydrogel Swelling and Its Effects

Theory resulting in Equation (4), allows experimental determination of release mechanism from hydrogel matrices by examination of the diffusional exponent. The degree of polymer swelling which

occurs during release, $\Delta\text{Swelling}\%$, was measured at temperatures 25 and 37 °C, as shown in Figure 6. For both ions it was found that an appreciable change, $\Delta = 16\%$ to 23% , in $\text{Swelling}\%$ occurred for the preloaded hydrogels. This is expected as the preloaded discs begin in an un-hydrated state and subsequently are further away from equilibrium. Conversely, the post-loaded hydrogels demonstrated a minimal $\Delta\text{Swelling}\%$, $\Delta = -8\%$ to -2% , with only one, Calcium at 25 °C, having a statistically significant change ($p < 0.05$) in $\text{Swelling}\%$ during the release. Interestingly, a reduction in the $\text{Swelling}\%$ was observed for the post-loaded discs, which was unexpected since as $t \rightarrow \infty$, $\text{Swelling}\% \rightarrow 100\%$. The cause of this initial reduction is unknown; however, it is hypothesized that it may be due to the weight loss of the salts within the polymer matrix. Further experimentation needs to be performed to test this conjecture.

Figure 6. K^+ and Ca^{2+} releasing hydrogels' $\Delta\text{Swelling}\%$ for pre- and post-loaded release.



Statistical analysis of the composite values showed no difference between the diffusional exponents for pre- and post-loading methods, when potassium was the released ion. Since K^+ release was shown to be unaffected by polymer relaxation, this result is expected. For Ca^{2+} release, which did demonstrate polymer relaxation effects, interpretation of the diffusional exponent for pre- and post-loading can be used to glean insight to the relation between polymer swelling and relaxation. If n values were reduced for the post-loaded relative to the pre-loaded, it would have indicated the removal of polymer swelling phenomena removed the polymer relaxation effects on the release mechanism. Since this did not occur and the n values for post-loaded Ca^{2+} release exhibited values predicted by Case II type release, it is concluded that polymer relaxation and polymer swelling are two independent processes and only the former effects ion release. During polymer relaxation, polymer pendent groups reorganize to reduce mechanical strain and relieve complexation sites while in polymer swelling the mesoscopic structure of the polymer is changing to accommodate a high water content to balance osmotic and mechanical forces. The latter happens on a time scale much longer than ion release and subsequently does not play a contributing role in the release mechanism.

4. Conclusions

In this work the release profiles of K^+ and Ca^{2+} from zwitterionic, pHEMA based hydrogels were studied. The contribution of polymer relaxation, valence state and temperature to the diffusional exponent and rate constant were investigated. It was shown that ion charge played the most significant role in the mechanism of release. This is primarily caused by a weak interaction between divalent cations and polyelectrolyte anions forming polymer-ion complexation sites which govern release. This interaction is not observed for monovalent ions and subsequently the mechanism of release is different. Temperature dependence of the diffusional exponent was observed for calcium but not potassium. This is likely due to a transition between case II type and Fickian type release for calcium. The cause for the transition is the increase of thermal energy which disrupts the polymer-ion complex. It was additionally shown that K^+ diffusivity constants followed Arrhenius type activation with apparent activation energy of -19 ± 15 kJ/mol. Conversely, k_{KP} for Ca^{2+} did not demonstrate a temperature dependent relation. The apparent negative activation energy is not fully understood, but it is not due to diffusion or ion mobility. Temperature dependent polymer swelling is a proposed hypothesis for the negative apparent activation energy. Statistical analysis showed differences in the release rate constant for each ion. The observed values are much higher than for neutral molecules, and it is proposed that the increase is primarily due to electromigration. This work demonstrates the Korsymer-Peppas release equation is an adequate model for the prediction of ion release from zwitterionic hydrogels; however, the work has shown other factors such as electromigration may play a role in ion release from hydrogels. Mechanistic phenomena were investigated through the diffusional exponent further demonstrating the utility of the equation. While fundamental phenomena of ion release from hydrogels has been elucidated here, further mathematical and experimental investigation of this system will be required to produce a more complete theory involving electromigratory effects.

Acknowledgments

This work was supported by the US Department of Defense Peer Reviewed Medical Research Program (DoDPRMRP) grant PR023081/DAMD17-03-1-0172, by the Consortium of the Clemson University Center for Bioelectronics, Biosensors and Biochips (C3B) and by ABTECH Scientific, Inc. Josh Crunkleton is thanked for assistance with the statistical analysis and the BMOLE 403/603 class of 2013 is thanked for exploratory active learning experiences that lead to this publication.

Author Contributions

Anthony Guiseppi-Elie designed and supervised the experimental work and wrote the manuscript. A. Nolan Wilson co-designed and conducted experiments and co-authored the manuscript. Mark Blenner supervised the experiments.

Appendix

Figure A1. Calibration plots used to relate measure mV to [Ion] for Calcium (A) and Potassium (B). Experimentally determined slopes as a function of temperature for Calcium (C) and Potassium (D).

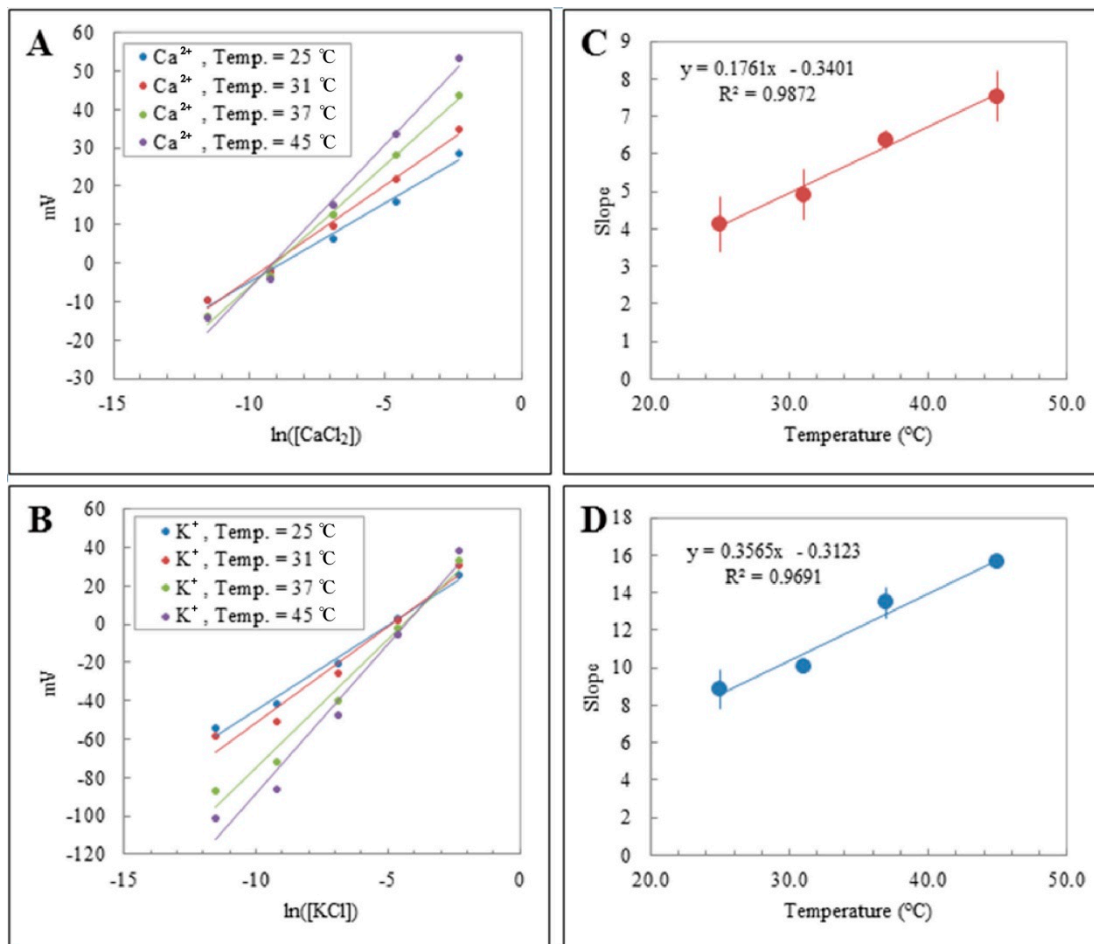


Figure A2. Predicted diffusion exponent as a function of aspect ratio for cylinders. Where *a* is radius and *l* is cylinder thickness. Reprinted with permission from [23].

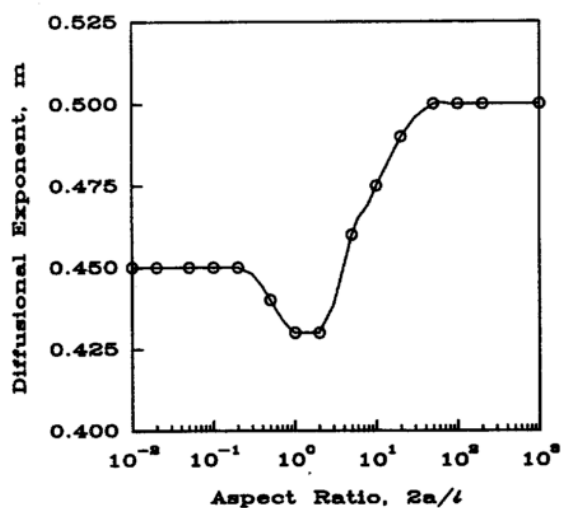


Table A1. Nested ANOVA setup for statistical analysis of ion (Factor A) and loading (Factor B) as main effects with Temperature as the nested variable for rate constant, k_{KP} , (**top**) and diffusional exponent, n , (**bottom**).

k_{kp} Rate Constant		Factor B												
		Preloaded						Postloaded						
Factor A	K ⁺	Temp = 25	0.163	0.308	0.151	0.163	0.130	0.079	0.169	0.231	0.294	0.167	0.287	0.114
		Temp = 31	0.385	0.077	0.134				0.148	0.084	0.084	0.182	0.096	0.144
		Temp = 37	0.037	0.100	0.133	0.100	0.077	0.048	0.180	0.158	0.093	0.123	0.193	0.170
		Temp = 45	0.190	0.115	0.094				0.104	0.084	0.168	0.183	0.096	0.067
	Ca ²⁺	Temp = 25	0.020	0.028	0.024	0.095	0.151	0.147	0.087	0.145	0.065	0.020	0.020	0.082
			0.082	0.088	0.076	0.098	0.025	0.096						
		Temp = 31	0.058	0.094	0.016	0.019	0.086	0.037	0.035	0.055	0.011	0.029	0.024	0.052
			0.020	0.167	0.021	0.063	0.145	0.040						
	Ca ²⁺	Temp = 37	0.105	0.065	0.065	0.050	0.032	0.087	0.135	0.076	0.173	0.020	0.022	0.035
			0.040	0.087	0.160	0.118	0.113	0.069						
		Temp = 45	0.086	0.055	0.076	0.073	0.065	0.007	0.061	0.036	0.025	0.003	0.033	0.011
			0.040	0.077	0.020	0.075	0.054	0.012						
n Exponent		Factor B												
		Preloaded						Postloaded						
Factor A	K ⁺	Temp = 25	0.33	0.19	0.35	0.33	0.38	0.49	0.29	0.25	0.19	0.44	0.19	0.44
		Temp = 31	0.11	0.55	0.39				0.28	0.42	0.43	0.27	0.41	0.30
		Temp = 37	0.68	0.40	0.40	0.42	0.45	0.54	0.30	0.27	0.42	0.35	0.36	0.32
		Temp = 45	0.30	0.41	0.45				0.35	0.38	0.26	0.24	0.38	0.42
	Ca ²⁺	Temp = 25	1.00	0.90	1.27	0.59	0.46	0.42	0.51	0.60	0.42	1.45	0.86	0.55
			0.53	0.48	0.67	0.46	0.81	0.61						
		Temp = 31	0.80	0.49	1.19	0.72	0.41	0.53	0.74	1.06	1.03	1.02	0.68	0.93
			0.85	0.31	0.69	0.59	0.33	0.60						
	Ca ²⁺	Temp = 37	0.44	0.62	0.58	0.63	0.93	0.63	0.66	0.59	0.38	1.02	1.12	1.64
			0.65	0.50	0.33	0.39	0.43	0.46						
		Temp = 45	0.43	0.60	0.50	0.36	0.45	0.84	0.82	0.64	0.64	1.09	0.71	1.32
			0.52	0.38	0.60	0.39	0.46	0.69						

Conflicts of Interest

The authors declare no conflict of interest.

References

1. Ottenbrite, R.M.; Park, K.; Okano, T. *Biomedical Applications of Hydrogels Handbook*, 1st ed.; Springer: New York, NY, USA, 2010; p. 700.
2. Brahim, S.; Narinesingh, D.; Guiseppi-Elie, A. Synthesis and hydration properties of pH-sensitive, p(HEMA)-based hydrogels containing 3-(trimethoxysilyl)propyl methacrylate. *Biomacromolecules* **2003**, *4*, 497–503.
3. Porter, T.; Stewart, R.; Reed, J.; Morton, K. Models of hydrogel swelling with applications to hydration sensing. *Sensors* **2007**, *7*, 1980–1991.

4. Phelps, E.A.; Enemchukwu, N.O.; Fiore, V.F.; Sy, J.C.; Murthy, N.; Sulchek, T.A.; Barker, T.H.; García, A.J. Maleimide cross-linked bioactive PEG hydrogel exhibits improved reaction kinetics and cross-linking for cell encapsulation and *in situ* delivery. *Adv. Mater.* **2012**, *24*, 64–70.
5. Abraham, S.; Brahim, S.; Ishihara, K.; Guiseppi-Elie, A. Molecularly engineered p(HEMA)-based hydrogels for implant biochip biocompatibility. *Biomaterials* **2005**, *26*, 4767–4778.
6. Wichterle, O. Process for Producing Shaped Articles from Three-Dimensional. U.S. Patent 2976576 A, 28 May 1961.
7. Yoon, H.Y.; Koo, H.; Choi, K.Y.; Lee, S.J.; Kim, K.; Kwon, I.C.; Leary, J.F.; Park, K.; Yuk, S.H.; Park, J.H. Tumor-targeting hyaluronic acid nanoparticles for photodynamic imaging and therapy. *Biomaterials* **2012**, *33*, 3980–3989.
8. Choi, N.W.; Kim, J.; Chapin, S.C.; Duong, T.; Donohue, E.; Pandey, P.; Broom, W.; Hill, W.A.; Doyle, P.S. Multiplexed detection of mRNA using porosity-tuned hydrogel microparticles. *Anal. Chem.* **2012**, *84*, 9370–9378.
9. Bromberg, A.; Jensen, E.C.; Kim, J.; Jung, Y.K.; Mathies, R.A. Microfabricated linear hydrogel microarray for single-nucleotide polymorphism detection. *Anal. Chem.* **2011**, *84*, 963–970.
10. Wu, K.; Liu, J.; Johnson, R.N.; Yang, J.; Kopeček, J. Drug-Free macromolecular therapeutics: Induction of apoptosis by coiled-coil-mediated cross-linking of antigens on the cell surface. *Angew. Chem.* **2010**, *122*, 1493–1497.
11. Rustad, K.C.; Wong, V.W.; Sorkin, M.; Glotzbach, J.P.; Major, M.R.; Rajadas, J.; Longaker, M.T.; Gurtner, G.C. Enhancement of mesenchymal stem cell angiogenic capacity and stemness by a biomimetic hydrogel scaffold. *Biomaterials* **2012**, *33*, 80–90.
12. Guiseppi-Elie, A.; Brahim, S.; Narinesingh, D. A chemically synthesized artificial pancreas: Release of insulin from glucose-responsive hydrogels. *Adv. Mater.* **2002**, *14*, 743–746.
13. Kirschner, C.M.; Anseth, K.S. Hydrogels in healthcare: From static to dynamic material microenvironments. *Acta Mater.* **2013**, *61*, 931–944.
14. Hoffman, A.S. Stimuli-responsive polymers: Biomedical applications and challenges for clinical translation. *Adv. Drug Deliv. Rev.* **2013**, *65*, 10–16.
15. Wilson, A.N.; Guiseppi-Elie, A. Bioresponsive hydrogels. *Adv. Healthc. Mater.* **2013**, *2*, 520–532.
16. Wilson, A.N.; Guiseppi-Elie, A. Targeting homeostasis in drug delivery using bioresponsive hydrogel microforms. *Int. J. Pharm.* **2014**, *461*, 214–222.
17. Gordijo, C.R.; Koulajian, K.; Shuhendler, A.J.; Bonifacio, L.D.; Huang, H.Y.; Chiang, S.; Ozin, G.A.; Giacca, A.; Wu, X.Y. Nanotechnology-enabled closed loop insulin delivery device: *In vitro* and *in vivo* evaluation of glucose-regulated insulin release for diabetes control. *Adv. Funct. Mater.* **2011**, *21*, 73–82.
18. Kost, J.; Langer, R. Responsive polymeric delivery systems. *Adv. Drug Deliv. Rev.* **2012**, *64*, 327–341.
19. Qiu, Y.; Park, K. Environment-sensitive hydrogels for drug delivery. *Adv. Drug Deliv. Rev.* **2001**, *53*, 321–339.
20. Brandl, F.; Kastner, F.; Gschwind, R.M.; Blunk, T.; Teßmar, J.; Göpferich, A. Hydrogel-based drug delivery systems: Comparison of drug diffusivity and release kinetics. *J. Control. Release* **2010**, *142*, 221–228.
21. Wang, L.; Liu, M.; Gao, C.; Ma, L.; Cui, D. A pH-, thermo-, and glucose-, triple-responsive hydrogels: Synthesis and controlled drug delivery. *React. Funct. Polym.* **2010**, *70*, 159–167.

22. Korsmeyer, R.W.; Peppas, N.A. Effect of the morphology of hydrophilic polymeric matrices on the diffusion and release of water soluble drugs. *J. Membr. Sci.* **1981**, *9*, 211–227.
23. Ritger, P.L.; Peppas, N.A. A simple equation for description of solute release I. Fickian and non-Fickian release from non-swelling devices in the form of slabs, spheres, cylinders or discs. *J. Control. Release* **1987**, *5*, 23–36.
24. Peppas, N.A.; Sahlin, J.J. A simple equation for the description of solute release. III. Coupling of diffusion and relaxation. *Int. J. Pharm.* **1989**, *57*, 169–172.
25. Alfrey, T.; Gurnee, E.; Lloyd, W. Diffusion in glassy polymers. *J. Polym. Sci. C Polym. Symp.* **1966**, *12*, 249–261.
26. Hopfenberg, H.B.; Frisch, H.L. Transport of organic micromolecules in amorphous polymers. *J. Polym. Sci. B* **1969**, *7*, 405–409.
27. Aucoin, H.R.; Wilson, A.N.; Wilson, A.M.; Ishihara, K.; Guiseppi-Elie, A. Release of potassium ion and calcium ion from phosphorylcholine group bearing hydrogels. *Polymers* **2013**, *5*, 1241–1257.
28. Kotanen, C.N.; Wilson, A.N.; Wilson, A.M.; Ishihara, K.; Guiseppi-Elie, A. Biomimetic hydrogels gate transport of calcium ions across cell culture inserts. *Biomed. Microdevices* **2012**, *14*, 549–558.
29. Geise, G.M.; Freeman, B.D.; Paul, D.R. Sodium chloride diffusion in sulfonated polymers for membrane applications. *J. Membr. Sci.* **2013**, *427*, 186–196.
30. Watanabe, J.; Ishihara, K. Establishing ultimate biointerfaces covered with phosphorylcholine groups. *Colloids Surf. B* **2008**, *65*, 155–165.
31. Wallmersperger, T.; Ballhause, D.; Kröplin, B.; Günther, M.; Gerlach, G. Coupled multi-field formulation in space and time for the simulation of intelligent hydrogels. *J. Intell. Mater. Syst. Struct.* **2009**, *20*, 1483–1492.
32. Kang, B.; Dai, Y.-D.; Shen, X.-H.; Chen, D. Dynamical modeling and experimental evidence on the swelling/deswelling behaviors of pH sensitive hydrogels. *Mater. Lett.* **2008**, *62*, 3444–3446.
33. Guiseppi-Elie, A.; Dong, C.; Dinu, C.Z. Crosslink density of a biomimetic poly(HEMA)-based hydrogel influences growth and proliferation of attachment dependent RMS 13 cells. *J. Mater. Chem.* **2012**, *22*, 19529–19539.
34. Kotanen, C.N.; Wilson, A.N.; Dong, C.; Dinu, C.Z.; Justin, G.A.; Guiseppi-Elie, A. The effect of the physicochemical properties of bioactive electroconductive hydrogels on the growth and proliferation of attachment dependent cells. *Biomaterials* **2013**, *34*, 6318–6327.
35. Ishihara, K.; Ueda, T.; Nakabayashi, N. Preparation of phospholipid polymers and their properties as polymer hydrogel membranes. *Polym. J.* **1990**, *22*, 355–360.
36. Lang, W.; Zander, R. Physiological HEPES buffer proposed as a calibrator for pH measurement in human blood. *Clin. Chem. Lab. Med.* **1999**, *37*, 563–571.
37. Brannon-Peppas, L.; Peppas, N.A. Dynamic and equilibrium swelling behaviour of pH-sensitive hydrogels containing 2-hydroxyethyl methacrylate. *Biomaterials* **1990**, *11*, 635–644.
38. Flory, P.J.; Rehner, J., Jr. Statistical mechanics of cross-linked polymer networks I. Rubberlike elasticity. *J. Chem. Phys.* **1943**, *11*, 512–520.
39. Huggins, M.L. Some properties of solutions of long-chain compounds. *J. Phys. Chem.* **1942**, *46*, 151–158.
40. Flory, P.J.; Rehner, J., Jr. Statistical mechanics of cross-linked polymer networks II. Swelling. *J. Chem. Phys.* **1943**, *11*, 521–526.

41. Brannon-Peppas, L.; Peppas, N.A. Equilibrium swelling behavior of pH-sensitive hydrogels. *Chem. Eng. Sci.* **1991**, *46*, 715–722.
42. Hooper, H.H.; Baker, J.P.; Blanch, H.W.; Prausnitz, J.M. Swelling equilibria for positively ionized polyacrylamide hydrogels. *Macromolecules* **1990**, *23*, 1096–1104.
43. Horkay, F.; Tasaki, I.; Basser, P.J. Effect of monovalent-divalent cation exchange on the swelling of polyacrylate hydrogels in physiological salt solutions. *Biomacromolecules* **2000**, *2*, 195–199.
44. Horkay, F.; Tasaki, I.; Basser, P.J. Osmotic swelling of polyacrylate hydrogels in physiological salt solutions. *Biomacromolecules* **2000**, *1*, 84–90.
45. Lee, W.F.; Lee, C.H. Poly(sulfobetaine)s and corresponding cationic polymers: 3. Synthesis and dilute aqueous solution properties of poly(sulfobetaine)s derived from styrene-maleic anhydride. *Polymer* **1997**, *38*, 971–979.
46. Berlinova, I.V.; Dimitrov, I.V.; Kalinova, R.G.; Vladimirov, N.G. Synthesis and aqueous solution behaviour of copolymers containing sulfobetaine moieties in side chains. *Polymer* **2000**, *41*, 831–837.
47. Wang, T.; Wang, X.; Long, Y.; Liu, G.; Zhang, G. Ion-Specific conformational behavior of polyzwitterionic brushes: Exploiting it for protein adsorption/desorption control. *Langmuir* **2013**, *29*, 6588–6596.
48. Yoshihiro, K. Making phospholipid-type hydrogel for biomedical application with attention to crosslinking point. Ph.D. Thesis, Department of Materials Engineering, the University of Tokyo, Tokyo, Japan, 2004.
49. Alencar de Queiroz, A.A.; Gallardo, A.; San Román, J. Vinylpyrrolidone-*N,N*-dimethylacrylamide water-soluble copolymers: Synthesis, physical–chemical properties and proteic interactions. *Biomaterials* **2000**, *21*, 1631–1643.
50. Novikov, S. Charge-carrier transport in disordered polymers. *J. Polym. Sci. B* **2003**, *41*, 2584–2594.
51. Trongsatitkul, T.; Budhlall, B.M. Microgels or microcapsules? Role of morphology on the release kinetics of thermoresponsive PNIPAm-co-PEGMA hydrogels. *Polym. Chem.* **2013**, *4*, 1502–1516.